A ^{31}P and ^{1}H MAS NMR Study of Phosphate Sorption onto Calcium Carbonate

Z. R. HINEDI,*,[1] S. GOLDBERG,‡ A. C. CHANG,* AND J. P. YESINOWSKI†,[1,2]

*Department of Soils and Environmental Sciences, University of California, Riverside, California 92521;
‡USDA-ARS, U.S. Salinity Laboratory, 4500 Glenwood Drive, Riverside, California 92501; and
†Division of Chemistry and Chemical Engineering, California Institute of Technology, Pasadena, California 91125

Received September 16, 1991; accepted November 18, 1991

The sorption of inorganic phosphate by two calcium carbonates, characterized by specific surface areas equivalent to 0.37 and 22 $m^2\ g^{-1}$, is studied using ^{1}H and ^{31}P MAS NMR spectroscopy. The ^{31}P MAS and CP-MAS NMR spectra of the low-phosphate-concentration (0.79 μmol P sorbed g^{-1} $CaCO_3$) sample show that the sorbed phosphate is most likely unprotonated, but the ^{31}P nucleus has a dipolar coupling to nearby protons. At this low concentration, the sorbed phosphate is not in the form of hydroxyapatite, nor does its spectrum resemble the ^{31}P CP-MAS NMR spectra of amorphous calcium phosphates previously characterized by other investigators. The solid state ^{31}P NMR spectra of samples with 3.33–36.72 μmol P sorbed g^{-1} $CaCO_3$ suggest the formation of a carbonated, apatitic-like phase. At phosphate addition levels that exceeded the computed monolayer coverage on the calcium carbonate surface, an apatitic-like phase and brushite were detected using ^{31}P CP-MAS NMR. The ^{1}H MAS NMR spectra of the phosphorus-free, high-surface-area synthetic calcium carbonate sample show a peak at ca. 5 ppm due to physisorbed water and a sharp peak at 6.7 ppm that is tentatively assigned to HCO_3^- or Ca–OH at the surface. In the samples containing high levels of sorbed phosphate, the ^{1}H MAS NMR spectra exhibit the characteristic spectral features of brushite. The sorption of phosphate onto calcium carbonate is described by fitting the NMR-characterized, surface-sorbed P species using the constant capacitance model.

The sorption of ions from aqueous solution onto surfaces of sparingly soluble inorganic solids is a fundamentally important chemical reaction in nature. Traditionally, the sorption reaction is characterized by solubility and kinetic-rate measurements. It was, however, pointed out in a critical review of geochemical processes at mineral surfaces (1) that one should be wary of using such macroscopic approaches to describe essentially molecular phenomena, such as adsorption and surface precipitation. Although electron and X-ray powder diffraction methods can be used to identify crystalline surface precipitates, spectroscopic methods sensitive to local environments are needed to provide structural information on sorbed species that lack three-dimensional order. Vibrational and X-ray photoelectron spectroscopies have been widely used to study surface reactions (2). High-resolution solid-state nuclear magnetic resonance (NMR) techniques have also provided a valuable element-specific probe into the chemical structure of surface species (3 and references therein). Two particularly useful methods have been cross-polarization (CP), which enhances the sensitivity of detection, and magic-angle spinning (MAS), which provides high-resolution spectra of solids. Both NMR methods were used in the present study to examine

[1] To whom all correspondence should be addressed.

[2] Current address: Naval Research Laboratory, Code 6122, Washington, DC 20375-5000.

0021-9797/92 $5.00

phosphate sorbed on calcium carbonate surfaces.

The mechanisms responsible for specific sorption (i.e., adsorption and precipitation processes) have been extensively discussed in the scientific literature (4–6) and there is a large body of information pertaining specifically to reactions of inorganic phosphate with mineral surfaces (7–10). In laboratory studies, the chemical nature of surface-sorbed inorganic phosphate depends upon the conditions under which the sorption experiment is conducted (e.g., whether pH-statted or varying pH, whether or not Ca-statted, and the value of the initial phosphate concentration) and the characteristics of the sorbing surface (i.e., seed material). A unifying theory has been proposed by Brown and co-workers to describe the nature of colloidal, apatitic calcium phosphates of varying Ca/P molar ratios and varying degrees of crystallinity (11). This theory postulates that the seemingly nonstoichiometric phosphorus compounds commonly observed are all part of a continuum of interlayered octacalcium phosphate (OCP) and hydroxyapatite layers in differing proportions. In studying surface-sorption phenomena, it is important to consider the role of heterogeneous nucleation in forming the mineral phases in natural waters and in geochemical environments (6, 12). A critical concentration of crystal components corresponding to a two-dimensional solubility product must be exceeded on the surface before a nucleus is formed, with crystal growth taking place preferentially on kinks or other sites rather than on a planar surface (13).

The reactions of phosphate (P) with mineral surfaces have practical applications in soil science, limnology, and wastewater treatment that have been extensively investigated (8, 12, 14–17). Morse (18) reviewed the influence of the surface chemistry of calcium carbonate on the sorption of inorganic ions (e.g., Mn^{2+}, PO_4^{3-}) in natural water and concluded that the adsorption process onto calcium carbonate is influenced by epitaxial considerations and may lead to the formation of new surface phases. Griffin and Jurinak (19) hypothesized from the kinetics of the reaction of phosphate with calcite that heterogeneous nucleation of an amorphous or semicrystalline phase on the $CaCO_3$ surface was followed by an induction period during which apatite was formed. Their conclusions corroborate those of Stumm and Leckie (20), who, based on the kinetics of apatite formation on calcite, postulate that the reaction occurs in three steps: (1) chemisorption of P forming amorphous calcium phosphate (ACP); (2) slow transformation of ACP into apatite; and (3) crystal growth of apatite. In contrast, solubility data (21) suggest that dicalcium phosphate dihydrate (brushite) is formed initially and slowly changes into OCP. Other studies, also based on solubility measurements, found that the phosphate in solution is in equilibrium with a surface complex, $Ca_3(HCO_3)_3PO_4$ (22, 23). Suzuki *et al.* (24), using labeled ^{32}P as the tracer, found that unprotonated PO_4^{3-} was preferentially sorbed onto the calcite surface even at a solution pH where protonated phosphate species predominated in solution. House and Donaldson (8), studying the adsorption and coprecipitation of P on calcite, found no evidence of a distinct calcium–phosphate solid phase that controls the P solution composition.

Surface-complexation models based on molecular hypotheses and constraint equations have been in existence for several years (25). Phosphorus sorption on $CaCO_3$ may be modeled by the Langmuir (19) and Freundlich (24) adsorption isotherms. These isotherms, however, are empirical in nature and have serious limitations when describing sorption mechanisms (1, 26). Thermodynamic calculations of the solution equilibria indicate that Ca^{2+}, HCO_3^-, CO_3^{2-}, H^+, and OH^- are all potential-determining ions on calcium carbonate mineral surfaces (27). Other evidence suggests that, for $CaCO_3$ particles, the potential-determining ion system is a Ca/anion pair rather than H^+/OH^- (28). Cowan *et al.* (29) described phosphate adsorption on calcite us-

ing an exchange reaction, but they did not consider any potential determining ions for calcite.

A variety of physical methods have been applied to characterize the sorption of phosphate onto calcite or other inorganic solids. Scanning electron microscopy (SEM) suggested that only a small fraction of the calcite surface was covered by the sorbed P (21). The surface-sorbed P was thought to act as a nucleus for the clustering of the more basic calcium phosphate phase (19). X-ray diffraction (XRD), in general, can only detect crystalline phases where concentrations exceed approximately 2% by weight. With the P concentration encountered in adsorption studies frequently <20 μmol P, the solid phases formed are often poorly crystallized and below the detection limit of X-ray diffraction spectroscopy. House and Donaldson (8), using electron-probe microanalysis, were not able to draw any conclusions concerning the spatial distribution of P sorbed onto calcite because of the low P concentration. Infrared (IR) spectroscopy has been used to characterize bulk-phase synthetic and naturally-occurring calcium phosphates (30, 31), and more specifically, carbonate-substituted apatites (32–35). CIR-FTIR measurements were used to characterize phosphate complexes sorbed onto the surface of goethite (36). Stumm and Leckie (20) identified apatite on the surface of calcite using grazing-angle electron diffraction. As noted previously, they suggested that P sorption onto calcite occurs in three stages: specific adsorption, nucleation, and crystal growth.

NMR spectroscopy, which is both element-specific and sensitive to the local structure surrounding a nucleus, is a useful tool for studying phosphate sorption onto calcite. Both ^{1}H and ^{31}P MAS-NMR have been used to characterize bulk calcium phosphate phases, including hydroxyapatite, octacalcium phosphate, brushite, and amorphous calcium phosphate. The ability of ^{31}P CP-MAS NMR to distinguish protonated from unprotonated phosphate groups in a series of synthetic crystalline calcium phosphates has been demonstrated (37–39). Increasing protonation of the phosphate group tends to result in a more upfield isotropic chemical shift as well as a marked increase in the chemical-shift anisotropy, resulting in a marked increase in spinning sideband intensities. Furthermore, ^{31}P MAS-NMR studies of other inorganic phosphates have been reported (40–43), and correlations of isotropic chemical shifts and shift anisotropies with local structure have been discussed (42, 43). The local structure of amorphous calcium phosphates has been studied using ^{31}P CP-MAS NMR by Tropp *et al.* (44); their conclusions were confirmed by Belton *et al.* (45), who apparently were unaware of the earlier work. High-speed ^{1}H MAS-NMR has demonstrated the capability of distinguishing between various calcium phosphate phases and quantitating the hydrous species present; furthermore, the isotropic chemical shifts correlate well with the degree of hydrogen bonding (i.e., the acidity) of the proton (46). Beshah *et al.* (47) have used ^{13}C and ^{1}H MAS NMR to distinguish between various types of carbonate-substituted apatites, and Papenguth *et al.* (48) have used ^{13}C MAS NMR to characterize inorganic and biogenic calcium and other alkali metal carbonates.

MATERIALS AND METHODS

Materials

Two calcium carbonate samples with different surface areas were used in this study. The Multifex MM sample (Specific Surface Area (SSA) = 22 $m^2 g^{-1}$), abbreviated hereafter as MM, is a precipitated calcium carbonate supplied by Pfizer Minerals, Pigments, and Metal Division, New York, NY. The other calcium carbonate sample (SSA = 0.37 $m^2 g^{-1}$) (Lot No. SRM 915), designated hereafter as NBS sample, was obtained from the National Institute of Standards and Technology, formerly the National Bureau of Standards, in Washington, DC. Both calcium carbonate samples were identified by X-ray powder dif-

fraction as calcite polymorphs. Analytical grade monobasic and dibasic potassium phosphate from Mallinckrodt, Inc., Paris, Kentucky, were used for the sorption experiments.

Phosphorus Sorption Experiments

The MM calcium carbonate (0.5 g) was allowed to equilibrate with deionized water (10 ml) in 50-ml Teflon centrifuge tubes at 22°–25°C for 30 min. Different aliquots of KH_2PO_4 stock solution were added to the $CaCO_3$ suspension to make a series of concentrations ranging between 0 and 4000 μmol liter^{-1} P when the contents were brought to a volume of 20 ml with deionized water. The capped tubes were placed on a wrist-action shaker, shaken for 3 h and then centrifuged. The pH of the supernatant was measured, and the supernatant was collected and analyzed for Ca by atomic-absorption spectrometry (Model 5000 atomic absorption spectrophotometer, Perkin-Elmer Corp., Norwalk, CT) and for phosphorus by colorimetric determination (49), using a Bausch & Lomb Spectronic 1001 spectrometer. The pellets were resuspended in 5 ml of deionized water and then lyophilized. The NBS calcium carbonate sample was treated in the same manner, except that the experiments were conducted over a narrower range of P concentrations. Experiments were also carried out with the MM calcium carbonate, using a stock solution of K_2HPO_4 to yield higher initial and final solution pH.

Given the small volume ratio of solid to liquid in the $CaCO_3$–water slurry and the significant depletion of initially added solution phosphate, the amount of phosphate potentially precipitated from interstitial solution in the centrifuged pellet during lyophilization is negligible.

Diffuse Reflectance Fourier-Transform Infrared (DR FT-IR) Measurements

The samples were diluted to 5% by weight in KBr. The transmission FT-IR spectra of these samples were recorded with a Mattson Cygnus 100 spectrometer using a Praying Mantis diffuse-reflectance cell made by Harrick Scientific, Ossinning, NY. Five hundred scans were collected in the 400–4000 cm^{-1} region at 4 cm^{-1} resolution under purged conditions.

NMR Measurements

The NMR experiments seeking to characterize phosphate sorbed onto calcium carbonate were run on a Bruker AM-500 spectrometer equipped with a multinuclear MAS probe made by Doty Scientific Inc., Columbia, SC. The lyophilized samples were packed in 5-mm, high-speed sapphire rotors. A synthetic hydroxyapatite (HAP-N) (50) was used as a secondary chemical shift reference for both ^{31}P and ^{1}H to improve the reproducibility of the chemical shift measurements (±0.1 ppm). The ^{31}P chemical shift of the HAP-N is 2.8 ppm (with respect to 85% H_3PO_4) and the hydroxyl ^{1}H chemical shift of the HAP-N is 0.2 ppm (with respect to TMS). Full decoupler power (ca. 40 W) was used for CP-MAS experiments, and an AR-200 amplifier (nominal output 200 W) was used as the final stage for the ^{31}P channel, with an attenuator on the input to adjust the Hartmann–Hahn matching condition on a sample of brushite. Additional filters and quarter-wavelength lines were used to protect the receiver from overload. The Bruker microprogram CPMAS.AUR, incorporating spin–temperature inversion to eliminate signals not arising from a cross-polarization process, was used for the CP-MAS NMR experiments. The 90° proton pulse for the CP-MAS experiments was typically 7.4 μs and the relaxation delay was typically 4 s. The ^{31}P half-height linewidth of brushite was 0.9 ppm or less. Either brushite or HAP-N was used as a secondary chemical shift reference for ^{31}P, and the HAP-N was used as a secondary reference for ^{1}H MAS-NMR. For absolute quantitation of the ^{1}H MAS-NMR peaks, the DISNMR manual baseline correction was applied to peaks before integration. A ^{1}H MAS-NMR spectrum of the HAP-N was obtained under identical conditions, and the integrals of the

OH peak and its sidebands were used as references. Using the measured weights of both samples, the % H_2O in the surface samples was calculated, using the previously determined % H_2O for HAP-N (50). The term "% H_2O" refers to the hydrogen content of the sample assuming that all of the hydrogen could be driven off in the form of water; it can be converted to % H simply by dividing by nine.

Modeling of P Sorption onto Calcium Carbonate

The spectroscopic information obtained from ^1H MAS, ^{31}P MAS, and CP-MAS NMR characterization of the species sorbed onto calcium carbonate was used to describe the P sorption by $CaCO_3$ using the constant capacitance model. A similar approach has been previously used where phosphate species sorbed onto aluminum oxide were characterized by NMR and subsequently described by the constant capacitance model (51).

RESULTS AND DISCUSSION

It has long been assumed that adsorption processes involve rather "rapid" kinetics while "slow" kinetics are more likely characteristic of surface-precipitation mechanisms. A more accurate assessment, when sorption occurs in supersaturated solutions, is that several mechanisms operate simultaneously from the very beginning (6). Results of kinetic studies (8, 10) showed that approximately 80% of the P sorption was completed in the first 2 min after the addition of the KH_2PO_4 solution to the calcium carbonate suspension. Longer reaction periods (i.e., 48 h) did not produce any significant change in the amount of P sorbed. We chose a relatively short reaction time (3 h) to minimize any eventual heterogeneous nucleation of apatitic phases at the initial sorption sites. The induction period for this reaction depends greatly upon the carbonate/phosphate ratio, but it can take place in a matter of days (19). Corey (5) described the mechanism of P sorption on calcium carbonate as a nucleation involving dissolution of the adsorbent (i.e., calcium carbonate). Direct spectroscopic examinations of the surface-sorbed P phase(s) would allow verification of the proposed mechanisms of P sorption on calcium carbonate.

The concentrations of P on calcium carbonate surfaces and the pH of the equilibrated solutions are listed in Table I. The amounts

TABLE I

Sorption of Phosphate on Different Calcium Carbonates and at Different pH Conditions

μmol sorbed · g^{-1} CaCO3	μmol P Added L^{-1}	μmol P sorbed L^{-1}	Final pH
0.00/MM	0	0.00	8.40
0.39/MM	10	9.96	8.25
0.79/MM	20	19.82	8.11
1.52/MM	40	38.13	7.96
3.33/MM	100	83.29	7.39
7.46/MM	200	186.6	7.22
15.13/MM	400	378.3	7.10
36.72/MM	1000	918.1	6.83
69.92/MM	2000	1748	7.03
63.26/MM	2000	1581	7.50
128.22/MM	4000	3205	7.40
19.22/MM	2000	480.5	9.69
8.60/MM	1000	215.0	9.73
0.65/NBS	20	16.34	7.78
3.49/NBS	100	87.30	6.91

TABLE II

Monolayer Coverage Calculations onto Calcium Carbonate for Phases with Various Ca/P Ratios

Molar ratio Ca/P	Phase	Calcium carbonate	μmol P·L^{-1} $CaCO_3$	μmol P·g^{-1} $CaCO_3$[a]
1.67	HAP	MM	2763	111
	$Ca_{10}(PO_4)_6(OH)_2$	NBS	46.3	1.85
3	COM	MM	1529	61
	$Ca_3PO_4(HCO_3)_3$	NBS	25.6	1.02
	(22, 23)			
1.67	Type A CarHap	MM	2763	111
	$Ca_{10}(PO_4)_6(CO_3)$	NBS	46.3	1.85
2.25	Type B CarHap	MM	2039	81.5
	(33, 34)	NBS	34.1	1.37
	$Ca_9(PO_4)_4(CO_3OH)_2$			
2.22	Hydroxycarbonate apatite	MM	2066	82.6
	$Ca_{10}(PO_4)_{4.5}(CO_3)_{1.5}(OH)_{3.5}$	NBS	34.6	1.38

[a] Calculated for monolayer coverage (Assuming Ca ions in these phases occupy the same surface area as in calcite).

of P sorbed in terms of the fractional monolayer coverage for various calcium phosphates of different Ca:P ratios are calculated (Table II). These computations were carried out using a surface area of 20 Å^2 per Ca atom (52) on the rhombohedral cleavage face of calcium carbonate. The number of moles of calcium per unit area would be equivalent to 8.3×10^{-6} moles Ca·m^{-2}. For MM calcium carbonate, with a SSA equal to 22.1 m^2 g^{-1}, the amount of Ca in a monolayer is calculated to be 183.5 μmol Ca·g^{-1} $CaCO_3$ (or 4587 μmol Ca·liter^{-1}); the corresponding value for the NBS calcium carbonate (SSA = 0.37 m^2·g^{-1}) is 3.07 μmol Ca·g^{-1} $CaCO_3$ (76.8 μmol Ca·liter^{-1}). Except for those samples exposed to the highest phosphate concentration (4000-μmol·liter^{-1} P initial solution), the amounts of sorbed phosphate in all other phosphorus-treated MM calcium carbonate samples correspond to less than a monolayer coverage by the unprotonated calcium phosphate phases we considered in Table II. However, we have evidence (see the discussion of FT-IR and NMR data to be presented later) that two sorbed calcium phosphate phases, an apatitic phase and brushite, are present at about 70 μmol P·g^{-1}, a level that is lower than the computed monolayer coverage. It is therefore unlikely that the sorbed P on the surface of MM calcium carbonate forms a monolayer phase. We were, however, unable to detect the brushite on the surface of the NBS calcium carbonate sample containing 3.49 μmol P·g^{-1}. At equilibrium pH = 9.7, four times less P was sorbed onto the MM calcium carbonate than at comparable P additions at neutral pH (see MM/1000 and MM/2000 in Table I). The lower P sorption, we suspect, is due to the fact that the solubility of brushite increases with increasing pH (53).

DR FT-IR Experiments

Three phosphorus-treated MM calcium carbonate samples (0.79, 3.33, and 63.2 μmol P g^{-1} $CaCO_3$), exhibiting a broad range of P concentrations, were characterized by DR FT-IR (Fig. 1). The DR FT-IR spectrum of the phosphorus-free MM calcium carbonate (not shown) exhibits all of the bands which are characteristic of calcite. They include the

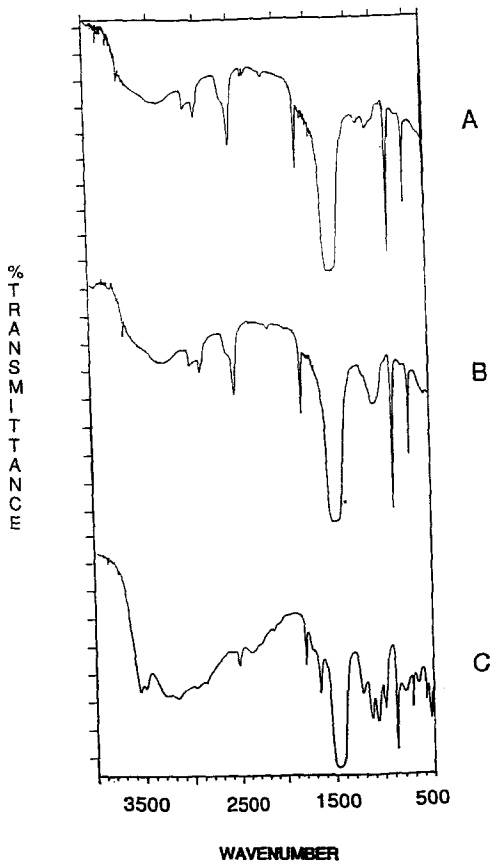

FIG. 1. FT-IR spectra of P sorbed onto calcium carbonate. (A) MM/0.79, (B) MM/3.33, and (C) MM/63.2.

broadband around 1410 cm^{-1}, which is derived from the stretching ν_3 mode of CO_3 and is common to all carbonates (seen in the spectra of the MM samples containing various levels of sorbed P in Fig. 1), and the bending ν_4 band around 710 cm^{-1} that distinguishes calcite from aragonite, which exhibits two bands (710 and 695 cm^{-1}) in this region (54, 55). The bicarbonate ion is strongly hydrogen bonded and the characteristic HCO_3 bands have been observed in the region of 2200–2500 cm^{-1} for $NaHCO_3$ and $KHCO_3$ (56). We therefore tentatively assign the band at 2500 cm^{-1} in Fig. 1 to HCO_3^- (see also evidence from ^1H MAS-NMR results to be presented later). The assignment of the bands at 2850 and 3000 cm^{-1} in Figs. 1A and B (and to a lesser extent, in Fig. 1C) is, however, uncertain. Hydroxyapatite is characterized by PO_4 modes that give rise to IR bands at ν_1 962, ν_3 1087, 1072–1032, ν_4 601, 571, and 474 cm^{-1}. The ν (OH) mode gives rise to bands at 3578 and 635 cm^{-1} in the IR region under study (50). In carbonate-substituted apatite, where CO_3 has partially replaced OH, ν (OH) bands are not always apparent in the IR spectra (32, 57).

At sorbed phosphate levels of 0.79 μmol P g^{-1} $CaCO_3$, the ν_3 bands characteristic of apatite at 1065 and 1090 are observed (Fig. 1A); however, the other apatite modes (ν_1 and ν_4) are missing. Those modes are probably associated with a more stoichiometric three-dimensional apatitic phase. At a phosphate-sorption level equal to 3.33 μmol P g^{-1} $CaCO_3$, additional bands related to apatite appear at 600 and 3600 cm^{-1}, while those due to PO_4 modes that were already present at the lower sorbed P concentration increase in intensity (Fig. 1B).

The brushite exhibits characteristic IR bands from PO_4 modes at ν_1 1000, 984, ν_3 1133, 1127, 1060, 1057 cm^{-1}, ν_4 580, 535, 530 cm^{-1}. Brushite also has additional bands from OH modes at ν_{OH} 3135–3539 cm^{-1}, δ_{OH} in plane 1215, 1200 cm^{-1} and ν_{POH} 870, 860 cm^{-1}, δ_{OH} out of plane 785 cm^{-1} (57). At 63.2 μmol P g^{-1} $CaCO_3$, IR bands characteristic of brushite appear at 785, 1000, 1080, 1130, 1220, 3500, and 3550 cm^{-1} (Fig. 1C). The IR evidence for brushite formation at the highest P-sorption level is supported by the NMR data to be presented later. The band at 1650 cm^{-1} is assigned to H–O–H bending of water.

^{31}P MAS and CP-MAS NMR Experiments

We will discuss here, sample-by-sample, the ^{31}P MAS and CP-MAS NMR results for the surface-treated calcium carbonate samples, since it is difficult to summarize some of the qualitative observations in Table III, and various experimental conditions were used. We

TABLE III

^{31}P and ^{1}H NMR Isotropic Chemical Shifts and Peak Assignments of Sorbed Phosphate on Calcite

Calcite/μmol P·g^{-1}	$\partial^{31}P$ (ppm)	^{31}P Peak assignment	$\partial^{1}H$ (ppm)	^{1}H Peak assignment
Multifex	—	—	5.6	Water
MM/0	—	—	6.7	HCO_3 or Ca-OH
			5.6	Water
MM/0.79	4.7	Unprotonated PO_4	6.65	HCO_3 or Ca-OH
			5.6	Water
			1.6	Organics
MM/3.33	3.3	Unprotonated PO_4		
MM/36.72	3.1	Unprotonated PO_4	6.6	HCO_3 or Ca-OH
			5.6	Water
			1.6	Organics
			≈0.2	OH
MM/69.92	3.7	Single pulse		
	3.7, 1.7	Cross polarization, mixture of unprotonated PO_4 & brushite		
MM/63.26			16	Acid phosphate
			10.7	Brushite
			6.6	HCO_3
			5.9	Water
			0.36, 1.1, 1.5	OCP/HAP or organics
MM/128.2			16	Acid phosphate
			10.7	Brushite
			6.6	HCO_3 or Ca-OH
			5.9	Water
			0.2, 1.1, 1.6	OCP/HAP or organics
NBS/0.65	3.1	Unprotonated PO_4		
NBS/3.49	3.1	Unprotonated PO_4	4.99	Occluded water
			5.6	Water
			0.2, 1.1, 1.5	OCP/HAP or organics

will also attempt to interpret the results in structural terms, drawing upon previously published work for crystalline and amorphous calcium phosphates (ACP) as summarized in Table IV. Since NMR spectroscopy, in general, is sensitive to the "local" environment (nearest and next-nearest neighbors, generally), there can be some ambiguity as to whether a particular form observed represents a distinct crystalline phase or something else. In particular, it is often difficult to distinguish between the four extreme conceptual possibilities of: (1) many unit cells of a crystalline compound, which may also contain substitutional impurities; (2) one or two unit cells (perhaps structurally distorted) of the same compound at a surface; (3) a chemisorbed form that does not resemble any known crystalline or bulk amorphous phase; and (4) a bulk amorphous form, lacking crystallinity as determined by X-ray powder diffraction and possessing variability in the local environments. Line-broadening of the NMR spectra is typical of amorphous materials, but also could occur in cases (2) and (3), if the local environments vary. Cross-polarization characteristics offer an additional means through which solid-state NMR spectroscopy offers the possibility of characterization of the local environment.

Since ACP is a possible form in which surface-precipitated phosphate could occur, it is

TABLE IV

^{31}P and ^{1}H NMR Chemical Shift Data for Selected Calcium Phosphates

Compound	^{31}P isotropic chemical shift	^{1}H isotropic chemical shift
Brushite (DCPD)	1.7 (37)	6.4, 10.4 (46)
$CaHPO_4 \cdot 2H_2O$		
Monetite	0.0, −1.5 (37)	16.2, 13.6 (46)
$CaHPO_4$	−0.3, −1.5 (39)	
Octacalcium phosphate	3.4 (37)	13.0, 0.2, 1.1, 1.5, 5.5 (H_2O) (46)
$Ca_8H_2(PO_4)_6 \cdot 5H_2O$	−0.1 (37)	
	1.7 (37)	
Hydroxyapatite	2.8 (37)	0.2, 5.5 (H_2O) (46)
$Ca_5(PO_4)_3OH$		
Carbonate apatite	3.0 (39)	NA
Type B (14.5% CO_3)		
Carbonate apatite	5.5, 4.6, 3.8, 2.5 (39)	NA
Type A		
Amorphous calcium phosphate	1.7 (44)	NA
$Ca_9(PO_4)_6 \cdot H_2O$	2.6 (45)	
	3.0 (39)	
β-Tricalcium phosphate	9.2, 5.2, 4.2 (45)	
$Ca_3(PO_4)_2$	5.1, 1.7, 0.6 (38)	

worthwhile to briefly discuss its ^{31}P MAS-NMR characteristics. Tropp *et al.* (44) observed a HHLW of 7 ppm, similar to the value we have observed for ACP at our higher field strength (5.5 ppm), and similar to values reported by Aue *et al.* (39) and Belton *et al.* (45). The isotropic chemical shift is determined less accurately than those for crystalline compounds, but from the various studies it appears to be the same as that of hydroxyapatite, possibly a few tenths of a ppm downfield. Tropp *et al.* (44) noted that the moderately weak sidebands of ACP did not change with CP contact time or between CP and single-pulse experiments, the latter observation being confirmed by Aue *et al.* (39). Belton *et al.* (45), who repeated these experiments and others on crystalline compounds while apparently unaware of the earlier papers, reported half-height line width (HHLW) values for ACP of both 4.4 ppm and 6.9 ppm, with no explanation for the differences. These researchers reported decreases in HHLW values upon aging of ACP precipitates, and between CP and single-pulse experiments, but it is not clear to what extent the samples remained amorphous. Carbonated ACP samples were also reported to have similar HHLW values of ca. 5 ppm. In summary, although there may

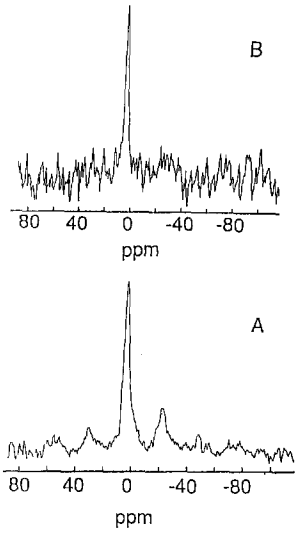

FIG. 2. ^{31}P MAS NMR spectra of sample MM/0.79: (A) Single pulse and (B) CP MAS. (See text for details).

be a range of compounds having molar Ca/P ratios ca. 1.5 that fall under the rubric "ACP," depending upon how the surface of the particles was washed, the degree of aging, etc., the ^{31}P spectral characteristics of all of these materials differ markedly from those of hydroxyapatite in having much broader line widths and more intense sidebands.

We will now discuss the surface-phosphate samples in order of increasing phosphate concentration for a given pH or surface area. The sample characterized by NMR containing the least sorbed phosphate on the MM calcium carbonate surface, MM/0.79 (Fig. 2), contains only 0.0025 wt% P atoms, and thus represents a challenge to the sensitivity of ^{31}P MAS-NMR. Nevertheless, by applying 40^0 pulses every 0.1 s without proton decoupling, reasonable sensitivity was obtained (Fig. 2A). Both the downfield chemical shift of 4.2 ppm and the low spinning sideband intensities (10–20% of the central peak at a spinning speed of 5.4 kHz) argue strongly against a protonated phosphate group. In an overnight CP-MAS spectrum (Fig. 2B) with a cross-polarization contact time of 3 ms, a weak peak is observed at 4.7 ppm, with a HHLW of 2.2 ppm, slightly narrower than the 3.2 ppm HHLW observed in a single-pulse spectrum. No sidebands are apparent in the CP-MAS spectrum. Thus, it appears that although the surface phosphate groups are not directly protonated, there are dipolar couplings to nearby protons, perhaps water molecules or bicarbonate groups (see below). However, the weakness of the CP signal relative to that in the single-pulse spectrum suggests that either the dipolar coupling is very weak or only a small fraction of the phosphate groups possess such a dipolar coupling. While the observed HHLW is greater than that observed for well-crystallized compounds, it is considerably less than the values reported for the amorphous calcium phosphates (see above paragraph). It is also less than the 5-ppm value reported for carbonated HAP by Aue *et al.* (39), although the chemical shift and increased sideband intensity relative to HAP are similar to those observed for carbonated HAP.

The MM/3.33 sample exhibits a slightly more upfield chemical shift (3.3 ppm) and a slightly broader HHLW of 4.0 ppm, both for a CP contact time of 3 ms and for a single-pulse spectrum (including the weak sideband intensities), confirming the lack of protonated phosphate groups.

The MM/36.7 sample continues this trend, with a chemical shift of 3.1 ppm and a HHLW of 4.4 ppm for a CP contact time of 3 ms. The weak sideband intensities point to a lack of directly protonated phosphate groups, although some dipolar coupling to protons must be present (no single-pulse spectrum was run for comparison).

At these lower phosphate concentrations, the results indicate that the surface phosphate groups are not protonated, but that at least some of them are dipolar coupled to nearby protons. The spectra differ from those of ACP, but may more closely resemble those from poorly crystalline HAP or carbonated HAP (although little ^{31}P CP-MAS NMR has been done on the latter) (39). As we increase the phosphate concentration, the MM/69.9 sample is the first to exhibit additional features (Fig. 3). The single-pulse spectrum with high-power decoupling obtained after a long relaxation delay of minutes (one scan) shows a single peak at 3.74 ppm with HHLW = 3.6 ppm and weak sidebands (Fig. 3A). However, the CP-MAS spectrum with a CP contact time of 0.5 ms and a spinning speed of 2.5 kHz differs markedly, having a sharp component with extensive spinning sidebands (Fig. 3B). The latter component is greatly deemphasized when the CP contact time is increased to 5 ms. The spectra arising from the individual components can be obtained by difference spectroscopy: the two spectra with different contact times are subtracted from one another in the DISNMR software by manually choosing the largest scaling factor for the spectrum being subtracted that avoids negative peak intensities in the difference spectrum. Thus, the sharper component is observed to have a chemical shift (1.7 ppm) and an intense spinning-sideband pattern characteristic of crystalline

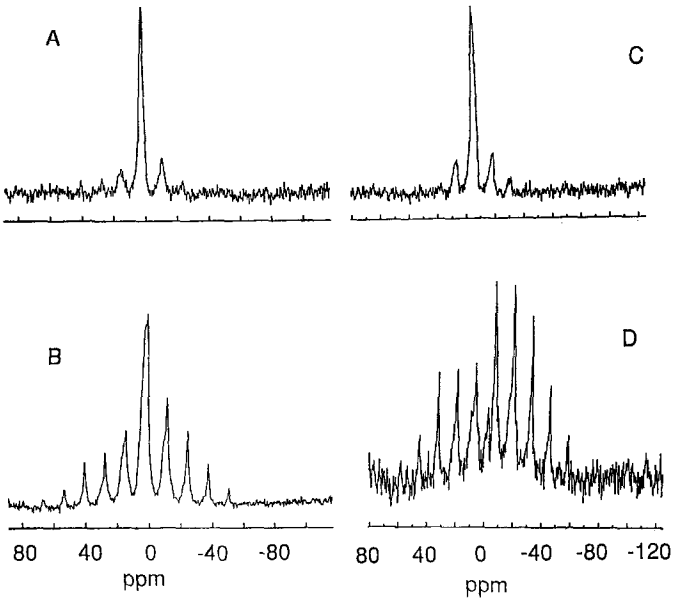

FIG. 3. ^{31}P MAS NMR spectra of sample MM/69.9: (A) Single pulse, (B) CP MAS, (C) difference spectrum (CP (0.5–5 ms)), and (D) difference spectrum (CP (5–0.5 ms)).

brushite ($CaHPO_4 \cdot 2H_2O$) (Fig. 3D). The broader component is thereby observed to have a chemical shift of 3.7 ppm and HHLW of 3.6 ppm and a pair of spinning sidebands that are each about 20% of the intensity of the center peak (Fig. 3C). This latter difference spectrum is very close to that of the single-pulse spectrum (Fig. 3A), which suggests that the brushite is a very minor component. Figure 3 is a graphic demonstration of how the cross-polarization process can result in a very unrepresentative view of a sample, and of the need to carry out a number of experiments involving single pulses and varying contact times. The linewidth and chemical shift of the major non-brushite component are intermediate between those observed for the MM/0.79 and MM/3.33 samples, and a similar assignment to unprotonated phosphate groups dipolar-coupled to nearby protons, perhaps apatitic in nature, can be made. The NBS calcium carbonate sample has a SSA that is 60 times less than that of the MM calcium carbonate, yet Table I shows that for a given initial concentration comparable amounts of phosphate are sorbed per gram of calcium carbonate. Such behavior is suggestive of surface precipitation rather than adsorption. The ^{31}P CP-MAS spectrum of NBS/0.65 with a CP contact time of 3 ms exhibits a peak at 3.1 ppm with a HHLW of 3.7 ppm and low relative sideband intensities. The corresponding spectrum of NBS/3.49 at a spinning speed of 3 kHz is similar: a single peak at 3.1 ppm with a somewhat narrower HHLW of 2.6 ppm and a pair of sidebands each about 25% of the intensity of the central peak. The chemical shift is thus nearly identical to that of the corresponding MM/3.33 sample, although the line width is somewhat less. As with the MM samples, we can conclude that the phosphate group in these low-surface-area samples is unprotonated but dipolar coupled to nearby protons, and that it may be apatitic in character. The MM calcium carbonate samples exposed to phosphate at high pH sorbed only about half as much as equivalent samples near neutral pH. House and Donaldson (8) observed an increased sorption at higher pH but for much lower levels of phosphate (less than 12 μmol). The ^{31}P

CP-MAS spectrum of MM/8.6 with a CP contact time of 3 ms is a very weak broad peak around 3 ppm. A single pulse spectrum at a spinning speed of 5 kHz and with a 4s relaxation delay shows in addition to this peak a sharper component at 1.3 ppm, both peaks having weak sidebands. The ^{31}P CP-MAS spectrum of MM/19.22 at a spinning speed of 3.8 kHz and a CP contact time of 3 ms has a chemical shift of about 1.8 ppm, a HHLW of 4.5 ppm, and sideband intensities relative to the center peak of about 30% and 16% for the right and left sidebands, respectively. The spectra of both of these high pH samples thus suggest that the phosphate group is unprotonated, although dipolar coupled to protons. In addition, in the lower concentration sample there may be phosphate groups (sharp peak at 1.3 ppm) that are not strongly dipolar coupled to nearby protons.

^{1}H MAS-NMR Experiments

The presentation of the ^{1}H MAS-NMR results will follow the same order of samples as that used for the ^{31}P NMR results. We will not discuss in any detail the peak from adsorbed water around 6 ppm in these samples, since its intensity and linewidth presumably depend upon the efficiency of the lyophilization process and any subsequent rehydration in the atmosphere. The ^{1}H MAS-NMR spectrum of the sample of "as is" MM calcium carbonate shows only a very broad peak around 6 ppm, which is due both to the physisorbed water and to the background signal of the probe (Fig. 4A). However, the same sample, after suspension in water, isolation, and lyophilization, exhibits an additional sharp peak at 6.7 ppm (HHLW approximately 0.3 ppm) and associated sidebands (Fig. 4B). (A weak absorption between 1.0 and 1.6 ppm may be attributed to organic contamination from handling the rotor, as noted by Yesinowski and Eckert (46).) At a spinning speed of 7.0 kHz the right and left first sidebands are 20% and 14% of the intensity of the centerpeak at 6.7 ppm, respectively. Since this peak is observed in the phosphate-treated samples as well, its assignment is important (Fig. 5A). The 6.7 ppm peak must arise from a surface species, since it only appears after the sample is suspended in water and dried, and since it is not observed after identical treatment of the low SSA calcium carbonate sample from NBS. The peak must arise from protons in a specific environment, since its linewidth is so narrow. The ab-

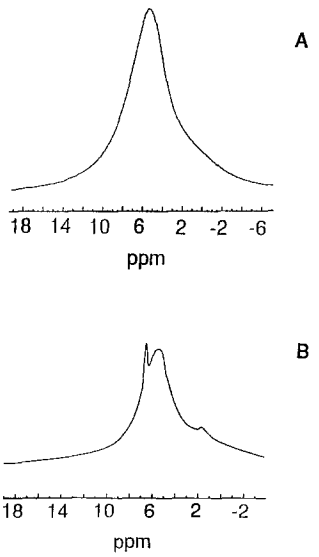

FIG. 4. ^{1}H MAS NMR spectra: (A) MM calcium carbonate and, (B) Washed MM calcium carbonate.

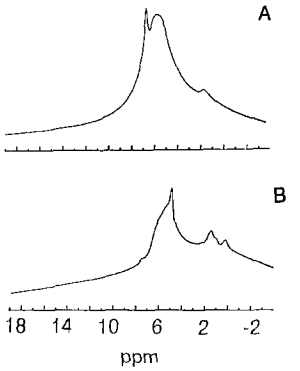

FIG. 5. ^{1}H MAS NMR spectra of P sorbed onto calcium carbonate: (A) MM/0.79 and (B) NBS 3.49.

sence of "dipolar sidebands," as observed for isolated water groups (58), argues against assignment to a tightly bound surface water molecule, which might be expected in any case to exchange with physisorbed water. The two most likely possibilities are a surface Ca-OH group or a surface bicarbonate ($H-CO_3$) group. Both groups would be expected to have a proton chemical shift anisotropy that would give rise to spinning sidebands. The chemical shift alone cannot be used to decide which possibility is correct, since proton chemical shifts depend directly on the degree of hydrogen bonding (and therefore, proton acidity), as discussed by Yesinowski *et al.* (58). Streaming potential measurements of the electrical state of the calcite/water interface in a closed system (containing no gas phase) over the pH range 7–10 have provided evidence against the existence of both HCO_3^- and $CaOH^+$ (28). The first and second pK values for carbonic acid in solution are 6.37 and 10.25 (59), but the corresponding values for the surface carbonate will be quite different. Arends *et al.* (50) (and references therein) have shown from the dissolution kinetics of hydroxyapatite that the acid dissociation constant of surface phosphate groups is some five orders of magnitude greater than that of solution orthophosphate (roughly half of the surface phosphate groups in HAP have been calculated to be monoprotonated at neutral pH). Unfortunately, similar calculations for the calcium carbonate surface do not appear to have been carried out. Another piece of evidence arises from the absolute quantitation of the ^1H peak at 6.7 ppm and its sidebands, which have an intensity in this sample corresponding to 0.076 wt.% H_2O. If we use the reported value of 20 $Å^2$/Ca atom on the cleavage face of calcium carbonate and the measured SSA of 22.1 $m^2 \cdot g^{-1}$, the result from the absolute quantitation corresponds to one proton (at 6.7 ppm) per 0.48 surface Ca atoms. Thus, the measured absolute intensity is reasonable for either possible assignment, if only one-half of the carbonate groups are in the form of bicarbonate, or one-half of the Ca atoms are in the form of Ca–OH. The assignment of the peak at 6.7 ppm to Ca–OH is not supported by the chemical shift value of 3.0 ppm measured for $Ca(OH)_2$ (H. Eckert, private communication), although differences in hydrogen-bonding could account for a difference. The ^1H chemical shift, δ_{iso} (in ppm), is correlated to the O–H · · · O distance, δ (in pm), by the following equation (58):

$$\delta_{iso} = 79.05 - 0.255\,\delta. \qquad [1]$$

If the resonance at 6.7 ppm is assigned to OH, this would predict an O–H · · · O distance of 283 pm, which is considered to be a moderately weak hydrogen bond. The OH stretching frequencies in IR studies are also related to hydrogen-bonding strength. White (60) showed that in $MgCO_3$ spectra a 3430 cm^{-1} band corresponds to a 287 pm O–H · · · O distance, while a 3610 cm^{-1} band corresponds to a 310 pm O–H · · · O distance. The FT-IR spectra (not shown) of selected samples in our experiment did not show any bands in the 3400 cm^{-1} region corresponding to the 283 pm O–H · · · O distance predicted from the proton NMR chemical shift. The expected IR band might be unobservably broadened by further hydrogen bonding to the water molecules observed to be present on the surface (the NMR peak might experience only an averaged hydrogen-bonding strength due to the slower time-scale of NMR compared to IR). Experiments using ^{13}C-labeling will be required to definitely establish the existence of surface bicarbonate.

Regardless of the assignment of the 6.7 ppm peak, it appears in the spectra of all the high SSA calcite (MM) samples treated with phosphate at neutral and high pHs except for one "aged" sample, but not in the low SSA sample (NBS) treated with phosphate. The spectra of individual samples are now described. The ^1H MAS-NMR spectrum of the MM/0.79 sample at an 8 kHz spinning speed (Fig. 5A) resembles that of washed MM calcium carbonate, with a sharp peak at 6.65 ppm, and a weak

shoulder at about 7.0 ppm. The right and left sideband intensities are 23 and 15% of the center peak intensity, similar to the washed MM calcium carbonate sample. No hydroxyl peak at 0.2 ppm from HAP (46) could be seen. It is likely that the peak at 6.65 ppm, attributed to a surface nonmobile proton, is responsible for cross-polarizing phosphorus in the CP-MAS experiments, rather than the more mobile protons of surface water molecules. Its sharpness and numerous sidebands (even at a low spinning speed (3.2kHz) (not shown)) reflect the inhomogeneous character of the broadening interaction, and the weakness of the dipolar interaction with other protons. The spectrum of MM/36.72 at a spinning speed of 7.7 kHz reveals some differences from the lower phosphate samples. The sharp peak at 6.68 ppm is still present, with right and left sideband intensities of 24 and 17%, but its absolute intensity corresponds to 0.049 wt% H_2O, about $\frac{2}{3}$ of the value for washed MM calcium carbonate. Some reduction in peak intensity relative to the starting sample would be expected as phosphate binds to the surface (see CCM discussion). In addition, there appear to be weak, poorly resolved "dipolar sidebands" associated with the broad central water peak at 5.6 ppm that extend over some 90 kHz. These sidebands are characteristic of hydrate water groups (58), and resemble those observed in ACP (J. P. Yesinowski, unpublished observations). Furthermore, there are three peaks at 1.55, 1.14, and 0.25 ppm which resemble those observed in certain samples of octacalcium phosphate (46). However, the 1.55 and 1.14 ppm peaks might also arise from organic contamination (see above). The quantitation of the 0.25 ppm peak yields a value of 0.0064 wt% H_2O, about one-eighth of the 6.68 ppm peak intensity. If we were to assume that all of the sorbed phosphate was in the form of stoichiometric HAP, we would calculate the OH group of HAP to be present at 0.011 wt% H_2O, roughly twice the observed intensity of the 0.25 ppm peak. Given the tendency of HAP to be substoichiometric in OH, and the large errors in quantitation, the quan-

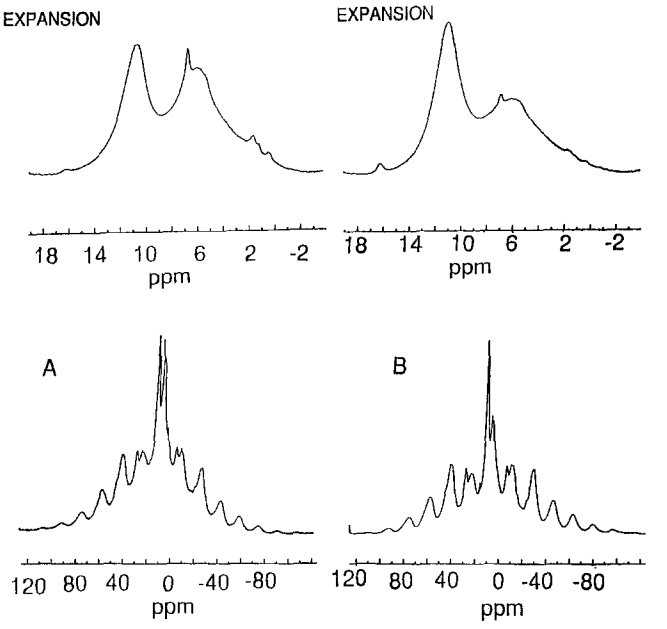

FIG. 6. ^1H MAS NMR spectra of P sorbed onto calcium carbonate: (A) MM/63.26 and (B) MM/128.2.

titative results for this sample support the existence of a hydroxyapatite-like form for the surface phosphate.

The ^1H MAS-NMR spectrum of MM/63.26 (Fig. 6A) at a spinning speed of 8.8 kHz clearly reveals the presence of brushite (Table IV), both by the acidic proton peak observed here at 10.7 ppm and by the hydrate water peak at 6.0 ppm with its associated dipolar sidebands. However, the 10.7 ppm peak appears to be considerably weaker relative to the dipolar sidebands than the corresponding brushite spectrum (46), suggesting that much of the hydrate water may arise from ACP. In addition, there are a sharp peak at 6.7 ppm whose area is 0.16% of the total spectrum, peaks at 1.5, 1.1, and 0.36 ppm whose area is 0.2% of the total spectrum, and a weak peak around 16 ppm whose area is 0.03% of the total spectrum. The latter probably corresponds to an acid phosphate proton, and the former peaks probably correspond to OCP/HAP or organic contamination.

The possible presence of solid-state transformations in surface samples upon lengthy aging should always be considered. The spectrum of an aged (6-month) sample at a similar phosphate concentration, MM/69.92, mainly shows a peak at 5.25 ppm with HHLW of 1.2 ppm and weak peaks at 1.5, 1.1, and 0.3 ppm having a quantitative intensity of 0.06 wt% H_2O. No dipolar sidebands or brushite peaks are observed. The ^{31}P CP-MAS spectrum of this sample, obtained much earlier, revealed the presence of brushite and an apatitic phosphate, but it appears that a solid-state transformation has occurred, resulting in a type of calcium phosphate containing few hydrous species. Like other samples exposed to high phosphate concentrations, the spectrum of MM/128.2 at a spinning speed of 8.8 kHz also reveals the presence of brushite, with the acidic phosphate at 10.7 ppm and the broad water peak and its associated dipolar sidebands (the ratio of these two types of protons agrees more closely with that observed for brushite than the previous sample). Again, the 6.7 ppm peak and a peak at 16.2 ppm are observed, along with three peaks between 1.6 and 0.2 ppm, with presumably the same assignments as for the MM/63.26 sample. The spectrum of the high pH sample MM/8.6 at a spinning speed of 7.4 kHz exhibits the sharp peak at 6.66 ppm with right and left sideband intensities of 19 and 15%, respectively, and with a quantitative intensity of 0.076 wt% H_2O. Since this last value is identical to that obtained for the corresponding peak in the washed MM calcium carbonate sample (neutral pH), it suggests that this peak may be due to surface Ca-OH rather than bicarbonate, which might be expected to be deprotonated at higher pH. In addition, there is an unusual set of peaks at 1.69, 1.47, 1.08, and 0.29 ppm with a quantitative intensity of 0.065 wt% H_2O, as well as a sharp peak at 16.2 ppm. We can only speculate as to possible assignments, but a downfield peak position (16.2 ppm) corresponding to strong hydrogen bonding is characteristic of an acidic group, and is unexpected under these basic conditions. The spectrum of the low SSA calcium carbonate sample NBS/3.49 has a new sharp peak at 5.0 ppm, which might be due to occluded water, as well as peaks at 1.5, 1.1, and 0.2 ppm with a quantitative intensity of 0.04 wt% H_2O. This value is surprisingly high, since it is similar to the corresponding result for MM/36.72, which has ten times the amount of sorbed phosphate. In this latter sample, a calculation suggested that the sorbed phosphate might be in the form of HAP containing only half the stoichiometric amount of OH. Possibly these peaks arise from species other than the ones considered.

Modeling of P Sorption on Calcium Carbonate Using the Constant Capacitance Model

The concentration of the phosphorus in its background solution was speciated using the chemical speciation model SoilChem and Ion Activity Products (IAP) were compared with solubility products of various calcium phos-

phate phases. Based on spectroscopic evidence obtained by ^1H MAS, ^{31}P MAS, and CP MAS NMR, P sorption on calcium carbonate results in the formation of an unprotonated surface CaP phase. The constant capacitance model is a surface complexation model which has been successfully applied to describe specific P sorption on metal oxide and hydroxide surfaces (25). Nuclear magnetic resonance results verified that phosphate adsorbs specifically on aluminum oxide, forming inner-sphere complexes (51). The initial adsorption mechanism for phosphate on calcite surfaces is considered to be chemisorption (20, 61, 62). Phosphate ions replace adsorbed water molecules, bicarbonate ions, and hydroxyl ions on the calcite surface (61). Specific adsorption of anions produces a shift in the zero point of charge (ZPC) of minerals to more acid values. A shift in ZPC was observed following phosphate adsorption on calcite, indicating specific adsorption (63). The constant capacitance model is based on the assumption that ion adsorption occurs specifically, forming inner-sphere complexes. The constant capacitance model assumes that the potential-determining ions for oxide minerals are H^+ and OH^-. The potential-determining ions for calcium carbonate are Ca^{2+}, HCO_3^-, and CO_3^{2-}, in addition to H^+ and OH^- (27). Surface complexation constants for the potential-determining ions of calcite have not yet been determined experimentally. Cowan *et al.* (29) described phosphate adsorption on calcite as an exchange reaction with carbonate and bicarbonate species. The formation constant for the carbonate surface species was arbitrarily fixed and the constant for bicarbonate surface species was determined by a fit to selenite adsorption data (29). Since the authors did not consider charges for surface complexes, no ions are considered to be potential-determining.

A rigorously correct representation of phosphate adsorption on calcite would consider the surface complexes of all potential-determining ions. Since these five surface complexation constants are not yet available experimentally, they must be considered as adjustable parameters, as in the study of (29) for carbonate and bicarbonate. In order to limit the number of adjustable parameters, we will consider only phosphate surface complexes in our study.

The surface reactions considered for P sorption on $CaCO_3$ are

$$2\text{–SOH} + H_3PO_4 \leftrightarrow S_2PO_4^- + H^+ + 2H_2O \quad [2]$$

$$SOH + Ca^{2+} + H_3PO_4 \leftrightarrow SPO_4Ca + 2H^+ + H_2O, \quad [3]$$

where SOH represents 1 mol of reactive surface hydroxyls bound to a Ca^{2+} ion (represented by S) in the calcium carbonate mineral. The above surface reactions are represented by the intrinsic conditional equilibrium constants

$$K_p^2(\text{int}) = \frac{[S_2PO_4^-][H^+]}{[SOH]^2[H_3PO_4]} \times \exp(-F\Psi/RT) \quad [4]$$

$$K_p^1(\text{int}) = \frac{[SPO_4Ca][H^+]^2}{[SOH][Ca][H_3PO_4]}, \quad [5]$$

where F is the Faraday constant, Ψ is the surface potential, R is the molar gas constant, T is the absolute temperature, and square brackets represent concentrations (mol liter^{-1}). The exponential term can be considered as a solid-phase activity coefficient that corrects for the charge on the surface species. The mass balance equation for the surface functional group, SOH, is

$$[SOH]_T = [SOH] + [S_2PO_4^-] + [SPO_4Ca] \quad [6]$$

and the surface charge equation is

$$\sigma = -[S_2PO_4^-], \quad [7]$$

where the units for surface charge are $mol_c \cdot liter^{-1}$.

TABLE V

Stoichiometry of the Equilibrium Problem

Species	Components							log K
	SOH	$e^{-F\Psi/RT}$	K^+	Ca^{2+}	H_2CO_3	H_3PO_4	H^+	
H^+	0	0	0	0	0	0	1	0.00
OH^-	0	0	0	0	0	0	−1	−14.00
SOH	1	0	0	0	0	0	0	0.00
K^+	0	0	1	0	0	0	0	0.00
Ca^{2+}	0	0	0	1	0	0	0	0.00
H_2CO_3	0	0	0	0	1	0	0	0.00
H_3PO_4	0	0	0	0	0	1	0	0.00
$H_2PO_4^-$	0	0	0	0	0	1	−1	−2.15
HPO_4^{2-}	0	0	0	0	0	1	−2	−9.35
PO_4^{3-}	0	0	0	0	0	1	−3	−21.70
$CaH_2PO_4^+$	0	0	0	1	0	1	−1	−0.75
$CaHPO_4$	0	0	0	1	0	1	−2	−6.61
$CaPO_4^-$	0	0	0	1	0	1	−3	−15.24
HCO_3^-	0	0	0	0	1	0	−1	−6.36
CO_3^{2-}	0	0	0	0	1	0	−2	−16.69
$CaHCO_3^+$	0	0	0	1	1	0	−1	−5.24
$CaCO_3$	0	0	0	1	1	0	−2	−13.55
KH_2PO_4	0	0	1	0	0	1	−1	−2.20
$KHPO_4^-$	0	0	1	0	0	1	−2	−8.20
KPO_4^{2-}	0	0	1	0	0	1	−3	−19.80
$S_2PO_4^-$	2	−1	0	0	0	1	−1	4.48
SPO_4Ca	1	0	0	1	0	1	−2	−2.29

Surface charge is a linear function of surface potential,

$$\sigma = \frac{CSa}{F}\Psi, \qquad [8]$$

where C is the capacitance density ($F \cdot m^{-2}$), S is the surface area ($m^2 \cdot g^{-1}$), and a is the suspension density of the calcite ($g \cdot liter^{-1}$).

Charged surface functional groups and charged surface complexes create a long-ranged potential field from partially screened coulomb forces (64). Since phosphate adsorbs specifically and is therefore potential-determining on calcite (63), the charge on the surface complexes interacts with other charged surface species. Our study is the first to consider the charge on the phosphate surface complex in the equilibrium expression.

The computer program FITEQL (65) that contains the constant capacitance model was used to fit intrinsic phosphate surface constants to the experimental sorption data. Table V provides the stoichiometry for the complete equilibrium problem defined for our model application. The number of reactive sites, $[SOH]_T$, equals 8.3 $mmol \cdot m^{-2}$, the number of calcium ions on the cleavage face of calcium carbonate. The capacitance density was set at

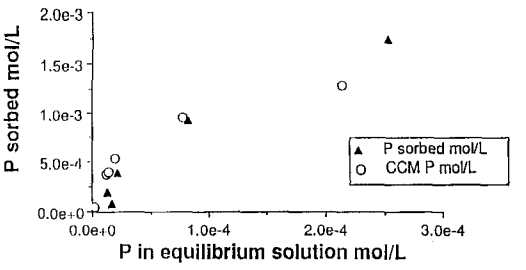

FIG. 7. Phosphorus sorption onto calcium carbonate described by the constant capacitance model.

$C = 8.0\ F \cdot m^{-2}$. The constant capacitance model was able to describe phosphate sorption over most of the phosphate concentrations (Fig. 7). It must be emphasized that in this model application, the only parameters optimized by the FITEQL program were log K_p^2 (int) and log K_p^1 (int). These two surface complexation constants represent unprotonated species that are in accord with the direct NMR evidence. We believe that the use of direct spectroscopic evidence to determine the type of surface complexes defined in the constant capacitance model is a useful approach that should be more widely applied.

SUMMARY

The results of the ^{31}P CP-MAS and the ^{1}H MAS NMR experiments on the P-treated calcium carbonate samples provide information that is complementary and confirmatory. Both methods show (along with XRPD not shown) the existence of crystalline brushite in calcium carbonate samples that are exposed to high phosphate levels. The important finding from the ^{31}P NMR that the surface sorbed P is an unprotonated calcium phosphate is supported by the lack of any ^{1}H NMR peak attributable to acid phosphate protons, except for the small peak at 16 ppm in the two highest concentration samples. The existence of protons that are dipolar coupled to phosphorus atoms of the unprotonated phosphate group, deduced from the presence of a ^{31}P CP signal, is consistent with the observation of a nonmobile proton species resonating at 6.7 ppm. The ^{1}H NMR characteristics of this peak provide some information about the nature and amount of this surface species: the constancy of its chemical shift and its relative sideband intensities in a wide range of samples argue for a well-defined and relatively unperturbed environment. Whether it arises from a surface bicarbonate group or a Ca–OH group remains to be determined. The nonprotonated character of the surface phosphate groups in forms other than that of brushite can be regarded as fairly firmly established by these results.

A more detailed structural specification of the sorbed phosphate is somewhat more problematic. The linewidths of the ^{31}P NMR signals appear to be too broad to attribute to a pure HAP phase, even for a poorly crystalline HAP (14). The ^{31}P NMR spectra of the variable CP contact time experiments of a P-treated MM calcium carbonate sample do not show the presence of octacalcium phosphate (OCP). Although the ^{1}H results for this sample did show some evidence of OCP, the complexities in the structural chemistry of OCP (46) make an unambiguous interpretation of the results difficult. The presence of amorphous calcium phosphate is also not supported by the results of the ^{31}P NMR experiments, because it has significantly broader peaks than those observed in the present study. However, the presence of both strong sideband intensities and a CP signal whose appearance does not depend upon the CP contact time are features shared by bulk amorphous calcium phosphate and at least some of the surface-sorbed phosphate species. In addition, the ^{1}H NMR data for some samples reveal the presence of nonmobile hydrate water similar to that observed in amorphous calcium phosphate. A further complicating factor is the possible presence of carbonate substitutions in the apatitic or amorphous forms of calcium phosphates. The attempt to identify the forms of P at a surface by comparison with features exhibited by model bulk compounds has its limitations, since only a small number of model bulk P compounds has so far been characterized by MAS-NMR techniques.

The spectroscopic NMR results do not appear to support the existence of the well defined $Ca(HCO_3)_3PO_4$ surface complex that was proposed by Avnimelech (22, 23), since no additional bicarbonate ^{1}H NMR peaks have been observed, and since the ^{31}P chemical shifts and linewidths change with increasing phosphate concentration. Further quantitative study of the ^{31}P CP-MAS NMR spectra using delayed-decoupling experiments (39) and extensive time-averaging will be required to better define the spatial proximity of the protons

responsible for the CP process. Both high-resolution ^{1}H and ^{31}P MAS-NMR have, nevertheless, provided a wealth of qualitative and, in some cases, quantitative spectroscopic information regarding the forms of phosphate sorbed to the calcite surface.

The constant capacitance model is able to fit the phosphorus sorption data using the unprotonated surface complexes as deduced from the NMR data. Based on the proportions of monodentate, SPO_4^-, and bidentate, S_2PO_4Ca, surface phosphate groups predicted by the constant capacitance model, a reduction of 0.042 to 0.062 wt% H_2O is expected. This agrees well with the water loss observed with the reduction in intensity of the ^{1}H NMR peak at 6.6 ppm when P is sorbed onto calcite. More refined NMR experiments on this surface system, including ^{13}C labeling and MAS of aqueous slurries, should be capable of providing additional information regarding the structural chemistry of sorbed phosphate, and help us to understand the mechanisms of this important process.

REFERENCES

1. Sposito, G., and Shindler, P. W., *in* "*Transactions of the 13th International Congress of Soil Science,*" Vol. **6**, p. 683. 1987.
2. Harsh, J. B., and Doner, H. E., *Geoderma* **36,** 45 (1985).
3. Yesinowski, J. P., and Mobley, M. J., *J. Am. Chem. Soc.* **105,** 6191 (1983).
4. Brener, R. A., "*Early Diagenesis.*" Princeton University Press, Princeton, NJ, 1978.
5. Corey, R. B., *in* "*Adsorption of Inorganics at Solid–Liquid Interfaces*" (M. A. Anderson and A. J. Rubin, Eds.), p. 161. Ann Arbor Science, Ann Arbor, MI, 1981.
6. Sposito, G., *in* "*Geochemical Processes at Mineral Surfaces*" (J. A. Davis and K. F. Hayes, Eds.), p. 217. ACS Symposium Series, No. 323, 1986.
7. Tomazic, B., and Nancollas, G. H., *J. Colloid Interface Sci.* **50,** 451 (1975).
8. House, W. A., and Donaldson, L., *J. Colloid Interface Sci.* **112,** 309 (1986).
9. Veith, J. A., and Sposito, G., *Soil Sci. Soc. Am. J.* **41,** 870 (1977).
10. Phelan, P. J. and Mattigod, S. V., *Soil Sci. Soc. Am. J.* **51,** 336 (1987).
11. Brown, W. E., Mathew, M., and Chow, L. C., *in* "Adsorption on and Surface Chemistry of Hydroxyapatite" (D. N. Misra, Ed.), p. 13. Plenum, New York, 1984.
12. Sherwood, B. A., Sager, S. L., and Holland, H. D., *Geochim. Cosmochim. Acta.* **51,** 1861 (1987).
13. Stumm, W., Furrer, G., and Kunz, B., *Croat. Chem. Acta.* **56,** 593 (1983).
14. Lindsay, W. L., and Moreno, E. C., *Soil Sci. Soc. Am. Proc.* **24,** 177 (1960).
15. Shukla, S. S., Syers, J. K., Williams, J. D. H., Armstrong, D. E., and Harris, R. F., *Soil Sci. Soc. Am. Proc.* **35,** 244 (1971).
16. Zoltek, J., Jr., *J. Water Pollut. Control Fed.* **46,** 2498 (1974).
17. Brown, J. L., *Soil Sci. Soc. Am. J.* **45,** 482 (1981).
18. Morse, J. W., *Mar. Chem.* **20,** 91 (1986).
19. Griffin, R. A., and Jurinak, J. J., *Soil Sci. Soc. Am. Proc.* **37,** 847 (1973).
20. Stumm, W., and Leckie, J. O., *in* "*Advances in Water Pollution Research,*" p. 1. Pergamon, Oxford, 1970.
21. Freeman, J. S., and Rowell, D. L., *J. Soil Sci.* **32,** 75 (1981).
22. Avnimelech, Y., *Nature (London)* **288,** 255 (1980).
23. Avnimelech, Y., *Limnol. Oceanogr.* **28,** 640 (1983).
24. Suzuki, T., Inomato, S., and Sawada, K., *J. Chem. Soc., Faraday Trans. 1* **82,** 1733 (1986).
25. Goldberg, S., and Sposito, G., *Soil Sci. Soc. Am. J.* **48,** 779 (1984).
26. Sposito, G., *Crit. Rev. Environ. Control* **15,** 1 (1985).
27. Somasundaran, P., and Agar, G. E., *J. Colloid Interface Sci.* **24,** 433 (1967).
28. Thompson, D. W., and Pownall, P. G., *J. Colloid Interface Sci.* **131,** 74 (1989).
29. Cowan, C. E., Zachara, J. M., and Resh, C. T., *Geochim. Cosmochim. Acta* **54,** 2223 (1990).
30. Chapman, A. C., and Thirlweill, L. E., *Spectrochim. Acta, Part A* **20,** 937 (1964).
31. Petrov, I., Soptrajanov, B., Fuson, N., and Lawson, J. R., *Spectrochim. Acta, Part A* **23A,** 2637 (1967).
32. LeGeros, R. Z., LeGeros, J. P., Trautz, O. R., and Klein, E., *Experientia* **24,** 5 (1969).
33. Bonel, G., *Ann. Chim. (Paris)* **7,** 65 (1972).
34. Bonel, G., *Ann. Chim. (Paris)* **7,** 127 (1972).
35. Chickeur, N. S., Tung, M. S., and Brown, W. E., *Calcif. Tissue Int.* **32,** 55 (1980).
36. Tejedor-Tejedor, M. I., and Anderson, M. A., *Langmuir* **6,** 602 (1990).
37. Rothwell, W. P., Waugh, J. S., and Yesinowski, J. P., *J. Am. Chem. Soc.* **102,** 2637 (1980).
38. Rothwell, W. P., Ph.D. Dissertation. Massachusetts Institute of Technology, 1980.
39. Aue, W. P., Roufosse, A. H., Glimcher, M. J., and Griffin, R. G., *Biochemistry* **23,** 6110 (1984).
40. Bleam, W. F., Pfeffer, P. E., and Frye, J. S., *Phys. Chem. Miner.* **16,** 809 (1989).
41. Griffiths, L., Root, A., Harris, R. K., and Packer, K. J., *J. Chem. Soc. Dalton Trans.* 2247 (1986).

42. Turner, G. L., Smith, K. A., Kirkpatrick, R. J., and Oldfield, E., *J. Magn. Reson.* **70,** 408 (1986).
43. Cheetham, A. K., Clayden, N. J., Dobson, C. M., and Jakeman, R. J. B., *J. Chem. Soc. Chem. Commun.* 195 (1986).
44. Tropp, J., Blumenthal, N. C., and Waugh, J. S., *J. Am. Chem. Soc.* **105,** 22 (1983).
45. Belton, P. S., Harris, R. K., and Wilkes, P. J., *J. Phys. Chem. Solids* **49,** 21 (1988).
46. Yesinowski, J. P., and Eckert, H., *J. Am. Chem. Soc.* **109,** 6274 (1987).
47. Beshah, K., Rey, C., Glimcher, M. J., Schimizu, M., and Griffin, R. G., *J. Solid State Chem.* **84,** 71 (1990).
48. Papenguth, H. W., Kirkpatrick, R. J., Montez, B., and Sandberg, P. A., *Am. Mineral.* **74,** 1152 (1989).
49. Murphy, J., and Riley, J. P., *Anal. Chim. Acta* **27,** 31 (1962).
50. Arends, J., Christoffersen, J., Christoffersen, M. R., Eckert, H., Fowler, B. O., Heughebaert, J. C., Nancollas, G. H., Yesinowski, J. P., and Zawacki, S. J., *J. Cryst. Growth* **84,** 515 (1987).
51. Bleam, W. F., Pfeffer, P. E., Goldberg, S., Taylor, R. W., and Dudley, R., *Langmuir* **7,** 1702 (1991).
52. Hurlbut, C. S., Jr., and Klein, C., *in* "*Manual of Mineralogy (after James D. Dana)*" (C. S. Hurlbut, Jr. and C. Klein, Eds.) Wiley, New York, 1977.
53. Stumm, W., and Morgan, J. J., "*Aquatic Chemistry,*" 2nd ed. Wiley, New York, 1981.
54. Chester, R., and Elderfield, H., *Sedimentology* **9,** 5 (1967).
55. White, W. B., *in* "*The Infrared Spectra of Minerals*" (V. C. Farmer, Ed.) p. 227. Mineralogical Society, London, 1974.
56. Nakamoto, K., Margoshes, M., and Rundle, R. E., *J. Am. Chem. Soc.* **77,** 6480 (1955).
57. Ross, S. D., *in* "*The Infrared Spectra of Minerals*" (V. C. Farmer, Ed.), p. 383. Mineralogical Society, London, 1974.
58. Yesinowski, J. P., Eckert, H., and Rossman, G., *J. Am. Chem. Soc.* **110,** 1367 (1988).
59. "*CRC Handbook of Chemistry and Physics,*" 56th ed., CRC Press, Cleveland, 1976.
60. White, W. B., *Am. Mineral.* **56,** 46 (1971).
61. Kuo, S., and Lotse, E. G., *Soil Sci. Soc. Am. Proc.* **36,** 725 (1972).
62. Holford, I. C. R., and Mattingly, G. E. G., *Geoderma* **13,** 257 (1991).
63. Amer, F., Mahmoud, A. A., and Sabet, V., *Soil Sci. Soc. Am. J.* **49,** 1137 (1985).
64. Sposito, G., "*The Surface Chemistry of Soils.*" Oxford University Press, New York, 1984.
65. Westall, J. C., "*FITEQL:A Program for the Determination of Chemical Equilibrium Constants from Experimental Data.*" Department of Chemistry, Oregon State University, Corvallis, OR, 1982.